

Development of Multiplexing Strategies for Electron and Super-Resolution Optical Microscopy

by

Paul W. Tillberg
B.S. Electrical Engineering and Materials Science (2010)
University of California, Berkeley

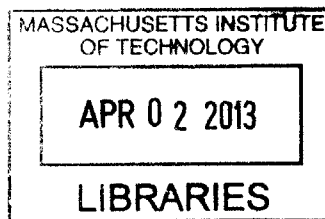
Submitted to the Department of Electrical Engineering and Computer Science
in Partial Fulfillment of the Requirements for the Degree of

Master of Science in Electrical Engineering and Computer Science
at the
Massachusetts Institute of Technology

February 2013

© 2013 Massachusetts Institute of Technology
All rights reserved

ARCHIVES



Signature of Author _____
Department of Electrical Engineering and Computer Science
January 22, 2013

Certified by _____
Edward S. Boyden
Associate Professor, MIT Media Lab
Thesis Supervisor

Accepted by _____
Leslie A. Kolodziejski
Chair, Department Committee on Graduate Students

Development of Multiplexing Strategies for Electron and Super-Resolution Optical Microscopy

by

Paul W. Tillberg

Submitted to the Department of Electrical Engineering and Computer Science
On January 22, 2013 in Partial Fulfillment of the
Requirements for the Degree of Master of Science in
Electrical Engineering and Computer Science

Abstract

The aim of this work is to increase the multiplexing capabilities of electron and super resolution optical microscopy. This will be done through the development of molecular-scale barcodes that can be resolved in one of the two high resolution imaging modes. In the optical domain, the number of colors available in stochastic optical reconstruction microscopy (STORM) will be increased by taking advantage of not only the spectral differences between STORM fluorophores but their kinetic properties as well. In the electron microscopy domain, the recently developed electron contrast-generating protein miniSOG will be concatenated to produce fully genetically encoded barcodes that can be resolved using standard transmission electron microscopy techniques. At the time of writing, the hardware for a STORM microscope has been assembled. Single molecule fluorescence blinking has been observed, though the imaging buffer still needs to be optimized for imaging. Concatamers of miniSOG have been generated and can be expressed in HEK cells and photo-oxidized.

Thesis Supervisor: Edward S. Boyden
Title: Assistant Professor, MIT Media Lab

Table of Contents

| | |
|--|----|
| 1. Introduction..... | 4 |
| 2. Background | 5 |
| 2.1. Genetically Encoded Electron Microscopy..... | 5 |
| 2.2. Multiplexed smFISH..... | 6 |
| 3. Multiplexing Genetically Encoded Electron Microscopy..... | 8 |
| 3.1. Design..... | 8 |
| 3.2. Cloning..... | 9 |
| 3.3. Photo-oxidation and Electron Microscopy | 13 |
| 3.4. Next Steps..... | 16 |
| 4. Highly Multiplexed STORM..... | 19 |
| 4.1. Strategies for Transcriptome-Scale smFISH | 19 |
| 4.2. Design and Construction of a STORM Microscope..... | 20 |
| 4.3. Single Molecule Fluorescence Characterization | 21 |
| 5. Conclusion | 26 |
| List of Figures | 27 |
| Appendix: Methods..... | 28 |
| References | 30 |

1. Introduction

Historically, electron microscopy (EM) has offered a level of spatial resolution orders of magnitude beyond what was possible with optical microscopy, due to the diffraction limit of roughly half the wavelength of light used to probe a specimen. Optical microscopy offered the possibility to easily label mRNA transcripts^{1,2} and proteins of interest, particularly with genetically encoded tools such as green fluorescent protein (GFP)³, and to label multiple such targets simultaneously with different colors of fluorescent molecule⁴. Recent advances in both fields have begun to bridge these differences. The genetically engineered proteins miniSOG⁵ and APEX⁶ promise a more straightforward approach to genetically encoding the labeling step in electron microscopy while stochastic optical reconstruction microscopy (STORM)⁷ techniques are bringing sub-10nm⁸ lateral resolution to optical microscopy. This work seeks to use the genetically encoded EM tools to enable multiplexing in electron microscopy, and to use STORM to enable highly multiplexed labeling in single molecule fluorescence *in situ* hybridization (smFISH).

Currently, multiplexed EM imaging requires the use of multiple antibodies with metallic nanoparticles of different sizes⁹. There are practical limitations to this technique, however, and it is rarely used with more than two labels. Quantifying double labeling immuno-EM data is challenging due to differential labeling of proteins by antibodies with differently sized nanoparticles¹⁰. Being able to determine the localization of multiple proteins simultaneously with EM-level resolution will add a critical dimension to existing techniques. For example, dopamine D1- and D2-type receptors have different responses to dopamine, and heterodimers of the two receptor types behave in a distinct way from either one alone¹¹. There are multiple known examples where the localization of a receptor in the middle *vs.* the periphery of a synapse strongly affects its function^{12,13,14,15}. Thus, the ability to localize multiple such proteins simultaneously at the EM-level will be an important tool in understanding the structure-function relationship of synapses.

Single molecule FISH using STORM has already been demonstrated with multiplexing of 32 distinct mRNA transcript probe sets¹⁶, but this is not enough to move the technology from fundamentally a hypothesis testing mode into an unbiased screen of a transcriptomic response to cellular stimuli. Existing transcriptomics techniques cannot detect

rare transcripts in a single cell context without homogenizing tissue and sacrificing all structural information¹⁷, while smFISH requires hypotheses that can be tested directly using a small number of specific transcripts¹⁸. A transcriptomics-scale approach to smFISH will combine the best of both techniques, enabling a qualitatively more complete picture of the state of a cell to be measured.

2. Background

This project relies on two recently developed technologies. Stochastic optical reconstruction microscopy (STORM), one of a number of super resolution optical microscopy techniques, has been developed to localize target molecules to within tens of nanometers in the lateral direction⁷, with recent advances pushing this limit to several nanometers⁸. This beats the traditional diffraction limit to resolution by more than an order of magnitude. This technique has been applied to single molecule FISH (smFISH) to multiplex the localization and measurement of 32 transcripts simultaneously¹⁶. MiniSOG and APEX are proteins, engineered from natural protein domains, that can be used to generate genetically encoded electron microscopy staining^{5,6}.

2.1. Genetically Encoded Electron Microscopy

Electron microscopy offers nanometer-scale spatial resolution, well beyond what is possible with super resolution optical microscopy. Even if super resolution techniques reach the resolution levels routinely achieved in electron microscopy, they require long image acquisition times and thus will not be readily scalable to collecting molecular-scale data over large structures. However, sample preparation procedures for EM are more involved and less readily adopted by labs that do not already practice them. Labeling proteins, a task that has been revolutionized in the optical domain by genetically-encoded tags such as EGFP, is generally done using antibodies in a technique called immuno-electron microscopy. Antibodies are expensive, and introduce a critical structure *vs.* antigenicity preservation tradeoff. In order to preserve nanometer-scale structural details, samples must be heavily fixed with high concentrations of glutaraldehyde. Through incompletely understood mechanisms¹⁹, this heavy fixation tends to reduce the ability of antibodies to bind their targets. Thus, EM studies typically must choose to focus on either elucidating ultra-structure or protein localization, but not both. This tradeoff is demonstrated in Maunsbach and

Afzelius²⁰, p. 385. Furthermore in pre-embedding immuno-EM, in which antibodies are delivered prior to resin embedding, the membrane must be permeabilized, resulting in an unavoidable direct degradation of cellular ultrastructure.

One way to avoid the ultra-structure *vs.* antigenicity tradeoff is with genetically encoded EM contrast agents. These have historically suffered from important limitations that prevent their widespread adoption. Horseradish peroxidase (HRP) is an enzyme that catalyzes oxidation of the small molecule diaminobenzidine (DAB) into a localized osmiophilic polymer that is readily stained using a standard EM osmium staining protocol²¹. A protein of interest can be labeled with HRP and subsequently localized in EM. However HRP, which is stabilized by several disulfide bonds, is rendered inactive in the reducing environment of the cytosol so the population of proteins that can be successfully localized in this way is limited⁶.

This limitation of genetically encoded EM has recently been overcome with two tools: mini-singlet oxygen generator (miniSOG)⁵ and an engineered variant of ascorbate peroxidase (APEX)⁶. APEX is an alternative to HRP that does not have any disulfide bonds and so can be used to localize proteins in any part of a mammalian cell. MiniSOG is a variant of the LOV2 domain of *Arabidopsis thaliana* phototropin 2. This light-sensitive protein was modified to maximize its production of singlet oxygen during illumination with blue light. Singlet oxygen then oxidizes DAB to form a localized polymer that can be stained using a standard osmium stain.

2.2. Multiplexed smFISH

In recent years an alternative technology has emerged for determining target localization beyond the diffraction limit of visible light—super-resolution optical microscopy. There are many approaches being developed in parallel to achieve this goal, and they fall broadly into two categories. In one, an effectively sub-diffraction limited fluorophore excitation beam (in practice a combination of excitation and de-activation or de-excitation) is rastered over the specimen. Stimulated emission depletion (STED) is one example of this approach²². In the other, an entire field of view is collected simultaneously. The second approach relies on the fundamental insight that the diffraction limit arises from the fact that in any real optical system, a point source of light in the specimen plane will produce a spot of finite extent (the point spread function) in the image plane. For any two

points closer together than the diffraction limit, the point spread functions overlap and the objects cannot be disambiguated. If, on the other hand, an isolated fluorophore creates a single such point spread function of illumination in the image plane, the center of that distribution can be determined to arbitrary precision, given a large enough number of photons²³. This fact is used in the second approach to super-resolution microscopy by using fluorophores that can be photo-switched between a light and dark state such that in any given video frame, no two activated fluorophores are within a diffraction limited spot of each other. Stochastic optical reconstruction microscopy (STORM)⁷ is one example of this approach, and is the focus of the super-resolution optical portion of this project.

Controlled photo-switching is usually accomplished through fluorophore pairs, where one acts as a ‘reporter’ whose fluorescence emission is recorded on a CCD. With the correct chemical environment, the reporter spontaneously switches to a dark state after emitting photons for a short time period. The second member of the fluorophore pair, the ‘activator’, is positioned within several nanometers of the reporter. After collecting fluorescence from one population of reporters, a specific fraction of them is re-activated through a FRET-like interaction when the associated activator is excited at its fluorescence absorption maximum. Thus two colors of light are required to see a given reporter: one to activate it and one to read it out. Activator and reporter pairs can be assembled combinatorially to yield increased numbers of effective colors. The actual numbers that can be achieved are limited by the specific performance of fluorophore pairs, but Bates *et al* have demonstrated five colors with negligible cross-talk by pairing Cy3 as an activator with Cy5, Cy5.5 and Cy7, and additionally using Alexa 405 and Cy2 as activators of Cy5²⁴.

Lubeck and Cai have extended this combinatorial approach to yield 35 distinct ‘colors’ in the context of highly multiplexed single molecule fluorescence *in situ* hybridization (smFISH)¹⁶. In this study, seven activator-reporter pairs were chosen with sufficiently low cross-talk. Three of the seven possible pairs were chosen and attached to probes for each mRNA transcript. There are a total of seven choose three, or 35, ways to do this, and thus the capability to distinguish 35 transcripts in the same specimen. As Lubeck and Cai point out, using one additional reporter in the near-IR range²⁵ would provide five additional ‘colors’ (by using the four activators already available for Cy5 plus Cy5 itself), bringing the maximum number of distinguishable codes to twelve choose five, or 792. If it were possible to distinguish the spatial order of colors appearing on each transcript, yielding a true

barcode, many more combinations would be distinguishable, but this approach did not prove to be robust enough to give reliable transcript identification.

3. Multiplexing Genetically Encoded Electron Microscopy

Multiple labeling can be achieved in immuno-EM by attaching different sized gold nanoparticles to antibodies against multiple targets. This project seeks to extend the capabilities of genetically encoded EM through a similar design. Concatamers of multiple miniSOG domains have been designed that will allow multiple proteins to be localized simultaneously. This technique may be extendable to large numbers of simultaneous labels by including spacing domains, or inactive miniSOG units, to produce an EM-resolvable barcode. In the multiple immuno-EM technique, antibodies with different sized-nanoparticles have different levels of access to their targets, but in this genetically encoded barcode approach, all labels will be identically sized and will be intrinsically attached to their targets.

3.1. Design

As a preliminary matter, it is important to determine roughly the size of the stained spot due to a single EM-contrast protein. This ‘point spread function’ will determine the minimum size of a bit in the final barcode design. If this size is too great, the barcode will simply not be usable. This can be done through a careful consideration of the single gap junction complexes imaged in the original miniSOG paper⁵. MiniSOG-labeled gap junctions made up of six connexin-43 proteins appear as approximately 10nm-wide stained spots. Based on the predicted structure of miniSOG, the protein occupies a space roughly 5nm in diameter, so the stained spot of a single miniSOG cannot be more than two times larger than a single miniSOG, and may be less if the imaged hemi-channels were composed of multiple miniSOG-labeled connexin-43 proteins. At this size, miniSOG is a promising tool for the construction of an EM-resolvable barcode.

Concatamers with six miniSOG repeats (6x-miniSOG) were designed by copying the amino acid sequence provided in the original miniSOG paper, with 15-residue polyproline linkers between them. Polyproline chains are thought to adopt a helical structure with a rise of 3 angstroms per amino acid, and a persistence length of at least 5nm²⁶. A 15-residue chain is then expected to form a rigid spacer about 4.5nm in length, equivalent roughly to the size of one miniSOG. The 6x-miniSOG amino acid sequence was provided to Genscript by

Nathan Klapoetke for codon optimization and cloning. The codons were varied between miniSOG repeats so as to reduce the risk of recombination due to tandem repeats at the DNA level.

3.2. Cloning

Single miniSOG and 3x-miniSOG tandem repeats were cloned using the codon-optimized sequences from 6x-miniSOG. Gibson assembly, a standard molecular biology technique²⁷, was used to stitch these pieces together without interposing unwanted restriction sites. All constructs were inserted into the pcDNA3.1(+) vector for mammalian expression using BamHI and EcoRV restriction sites. All restriction enzymes were purchased from New England BioLabs. All PCR reactions were conducted using Phusion polymerase from New England BioLabs using the manufacturer-recommended protocols.

All constructs were transfected into HEK293FT cells and resulted in expression of functional miniSOG, as judged by the presence of fluorescence. Using the calcium phosphate transfection protocol, transfection efficiency for 1x-miniSOG could be increased from approximately 10% to 50% by increasing the dose of plasmid from 12 to 75ng (total DNA including dummy pUC57 was 1.25ug) while the efficiency level for 6x-miniSOG was approximately 10% for both 12 and 75ng doses. Increasing the 6x-miniSOG dose to 75ng did result in a greater amount of perinuclear aggregation, suggesting that transfection of multiple copies of the plasmid is overwhelming the protein trafficking machinery. This would also explain why the apparent transfection efficiencies remain low, as over-expressing cells would not be able to grow and divide as quickly as non-expressing cells, reducing the apparent transfection efficiency after several rounds of cell division.

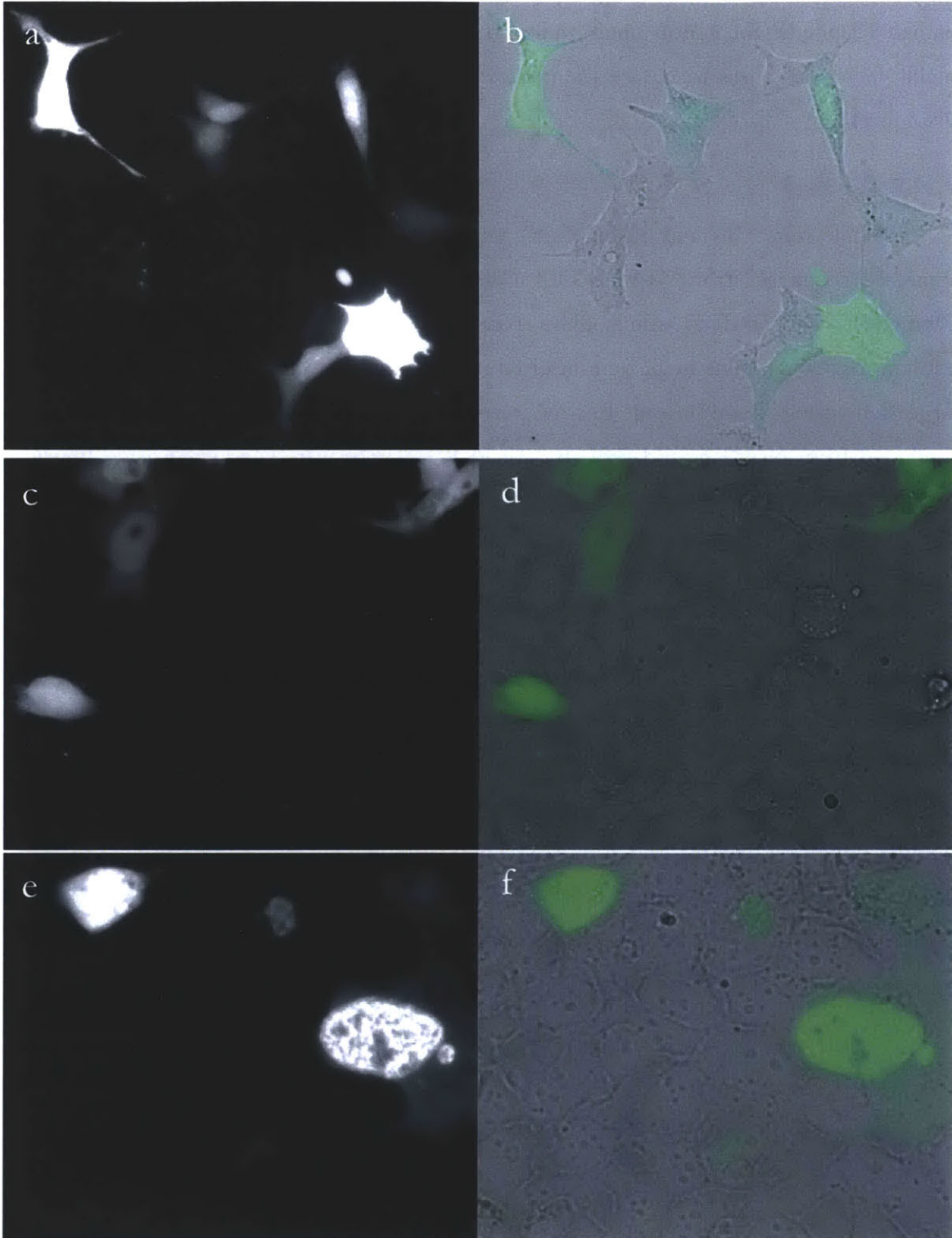


Figure 1. HEK293FT cells expressing miniSOG constructs. Fluorescence and bright field images of cells transfected with 75nm of 1x-miniSOG DNA (a, b), 12ng of 6x-miniSOG (c,d), and 75ng of 6x-miniSOG (e,f). Bright field images (b,d,f) include an overlay of the fluorescence intensity in green.

In addition to these cytosolically expressing miniSOG constructs, two approaches were tried to generate membrane-localized versions: fusion with the membrane-localized connexin-43 protein, and fusion with the trans-membrane domain of human major histocompatibility complex (MHC)-I. A membrane-localized version of the miniSOG concatamers will be useful in the barcode development phase of the project because they provide a distinct localization that can easily be distinguished in electron micrographs from cytosolic bodies such as ribosomes that are also stained by osmium tetroxide.

The connexin-43-miniSOG (Cx43-mS) fusions show signs of proper localization, but the rate of healthy cells expressing it is too low to be useful for the purposes of barcode development, in which hunting through a specimen with less than 5% transfection efficiency is not acceptable. In a study of Cx43-mS localization, fusion of connexin-43 and four constructs (1x-, 3x-, and 6x-miniSOG, and EGFP as a positive control) were transfected into HEK293FT cells using Lipofectamine and calcium phosphate (Cal Phos). Cal Phos transfections were carried out with three concentrations of construct DNA: 12ng, 75ng, and 500ng with pUC57 filler DNA added to reach 1.25ug of DNA for 24-well-plate well. The positive control (Cx43-EGFP) transfected using Lipofectamine showed the expected combination of punctate intracellular fluorescence corresponding vesicles transporting the protein through the endoplasmic reticulum and Golgi apparatus and dense membrane staining at the junction between neighboring cells (Figure 2, a and b). Cx43-1xmS, however, shows a high number of unhealthy cells, some indistinct intracellular labeling, and no clear membrane localization. Calcium phosphate transfection of these constructs resulted in healthier cells but also a much lower transfection efficiency, in the 1-5% range. Thus, the appropriate balance of cell health and transfection efficiency required for use as an aid in barcode design has not been found.

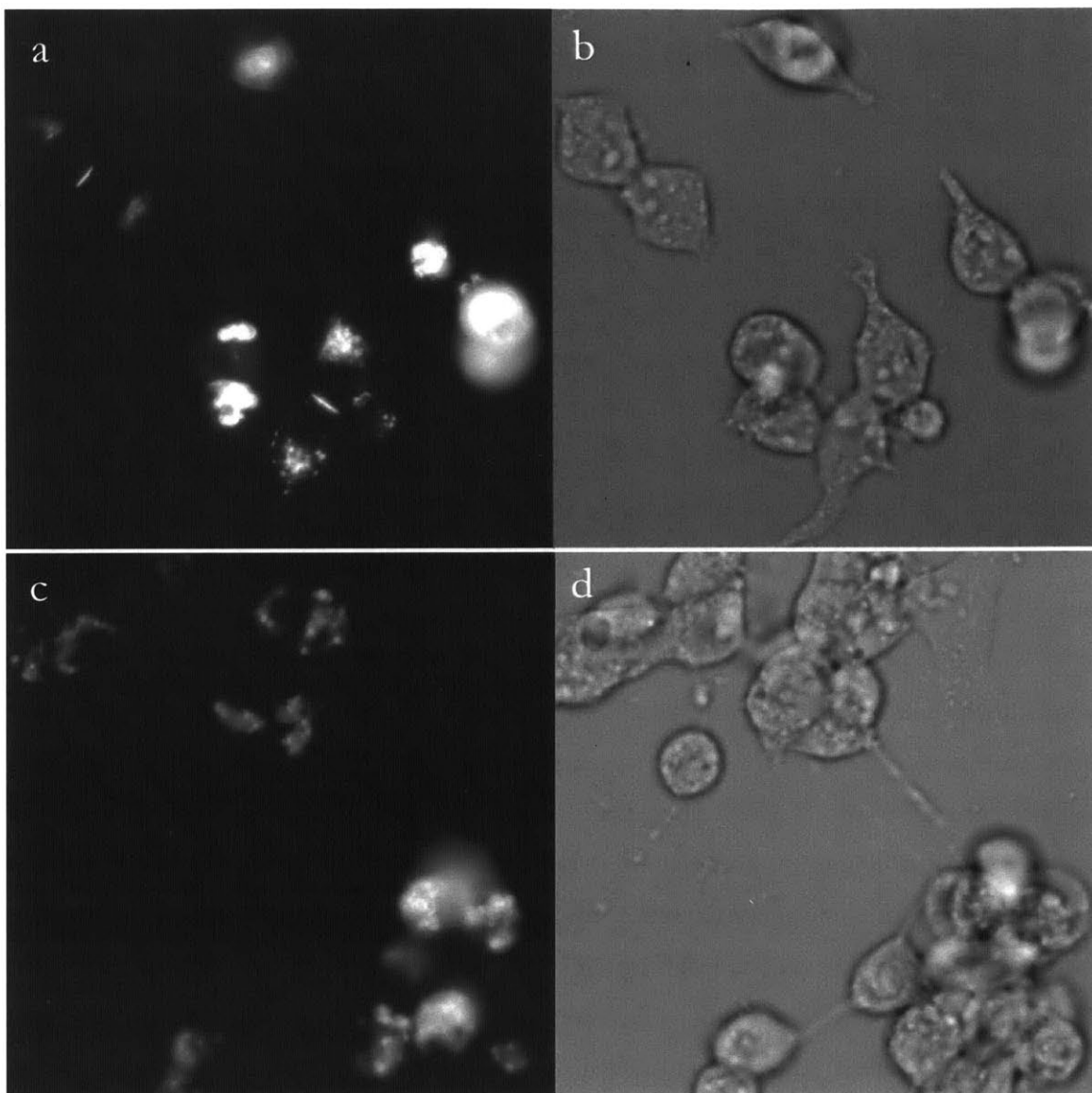


Figure 2. HEK293FT cells expressing fusions with connexin43. Fluorescence and bright field images of cells transfected with connexin43-EGFP (a,b) and connexin43-1x-miniSOG (c,d).

The fusion of MHC1 and 1x-miniSOG appeared to be more promising in terms of expression, though still not expressing at nearly the levels of non-membrane localized miniSOGs. However, the position of MHC1 as an extracellular membrane-bound protein is likely to be a fatal flaw for this fusion construct. As described below, the photo-oxidation of miniSOG requires the local environment to be heavily fixed with glutaraldehyde, or else the oxidized DAB diffuses freely throughout the buffer solution. Without the crowded, heavily fixed environment found inside the cell, extracellular miniSOG would then be expected not to produce an immobilized DAB reaction product.

3.3. Photo-oxidation and Electron Microscopy

The photo-oxidation procedure was carried out successfully on HEK cells expressing miniSOG cytosolically, as judged by the appearance of a dark brown reaction product. As expected, within several minutes of illumination with intense blue light in an inverted fluorescence microscope miniSOG fluorescence was reduced beyond the limit of visual detection, and several minutes thereafter the reaction product appeared only in cells displaying miniSOG fluorescence. Using the same procedure but omitting the strong fixation step resulted in no cell-confined staining but after prolonged light exposure did result in a general darkening of the buffer solution.

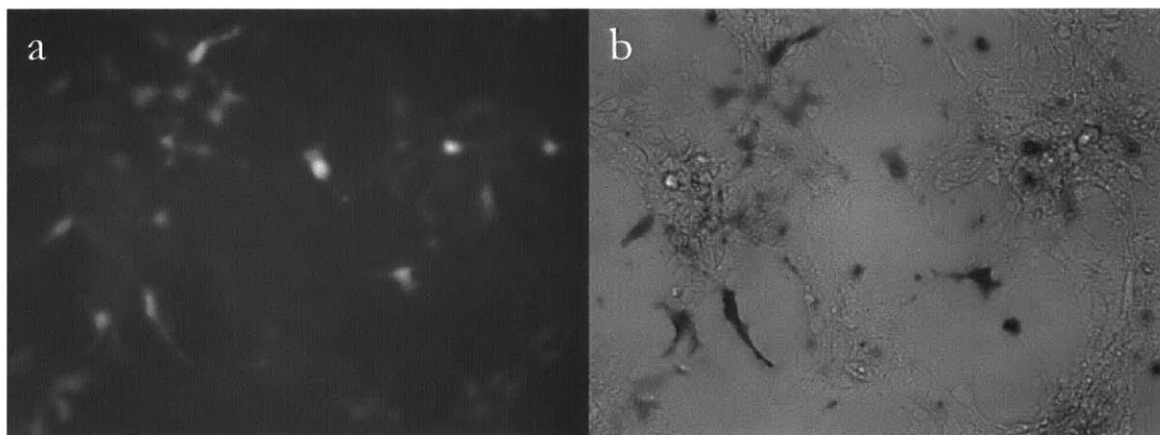


Figure 3. Photo-oxidation of 1x-miniSOG. Fluorescence of HEK293FT cells expressing 1x-miniSOG before photo-oxidation (a) and bright field after photo-oxidation (b).

All electron microscopy was performed by Nicki Watson at the Whitehead Institute Keck Microscopy Core. The results from the first round of electron microscopy are ambiguous. Dark spots about 20nm in diameter were detected in the 6x-miniSOG specimen, which would be expected based roughly on the size of the protein, but spots of similar size were observed in both the 1x-miniSOG and the negative control specimens. In the negative control, these spots are most likely due to ribosomes, which are also stained in the standard osmium staining protocol (osmium tetroxide followed by uranyl acetate and lead citrate for increasing contrast). This is in spite of the fact that for this experiment only osmium and uranyl *en bloc* staining were used. Usually, once specimens have been sliced ultra-thin and arranged on TEM grids, a second uranyl and lead stain is used to increase contrast but in this case, this contrast enhancing step was omitted. For these cytosolically expressing miniSOG constructs, there is no way to be sure whether any given spot is due to miniSOG or

ribosomes. Alternative approaches will be considered for completing this phase of the project.

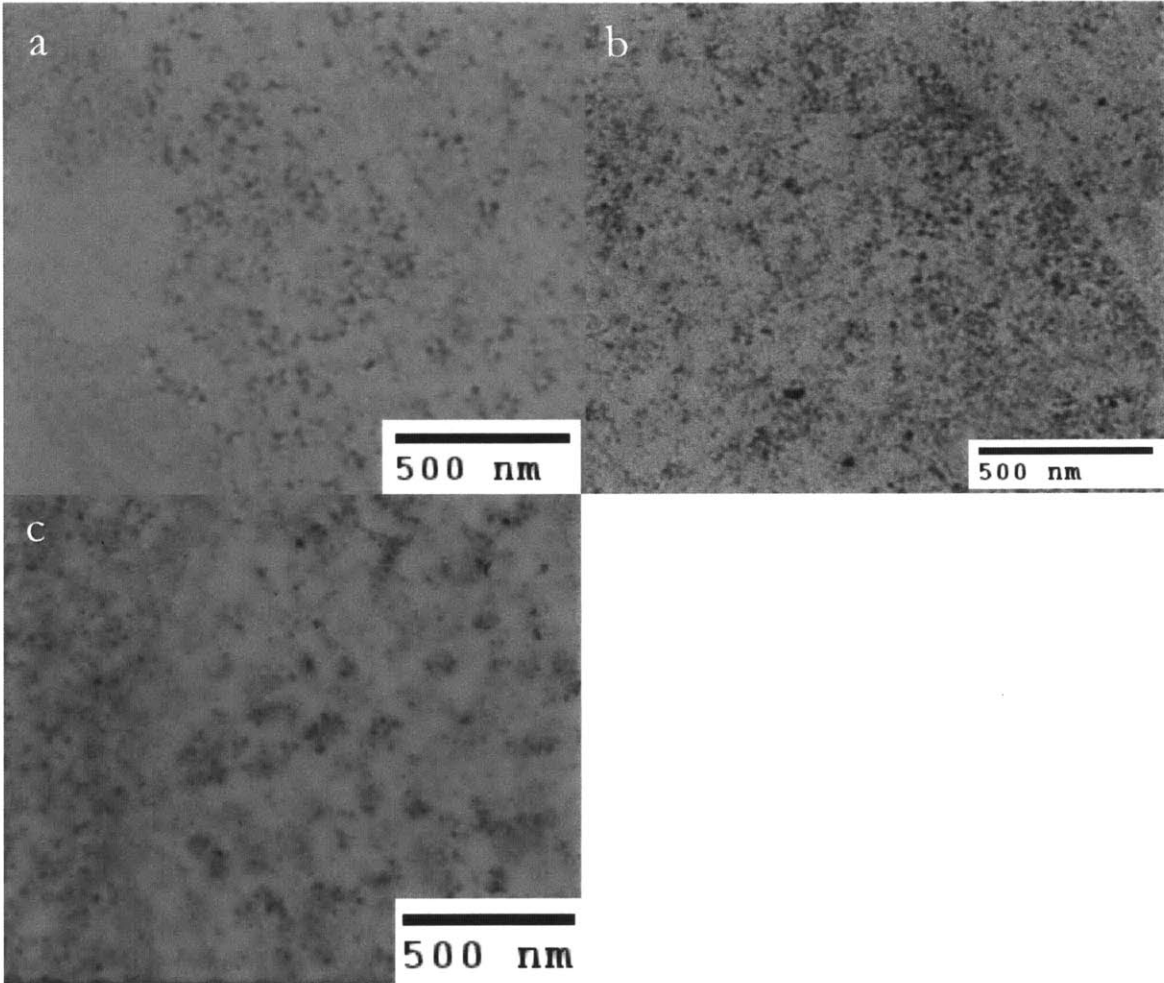


Figure 4. Transmission electron micrographs of HEK293FT cells expressing no miniSOG (negative control, a), 1x-miniSOG (b), and 6x-miniSOG (c).

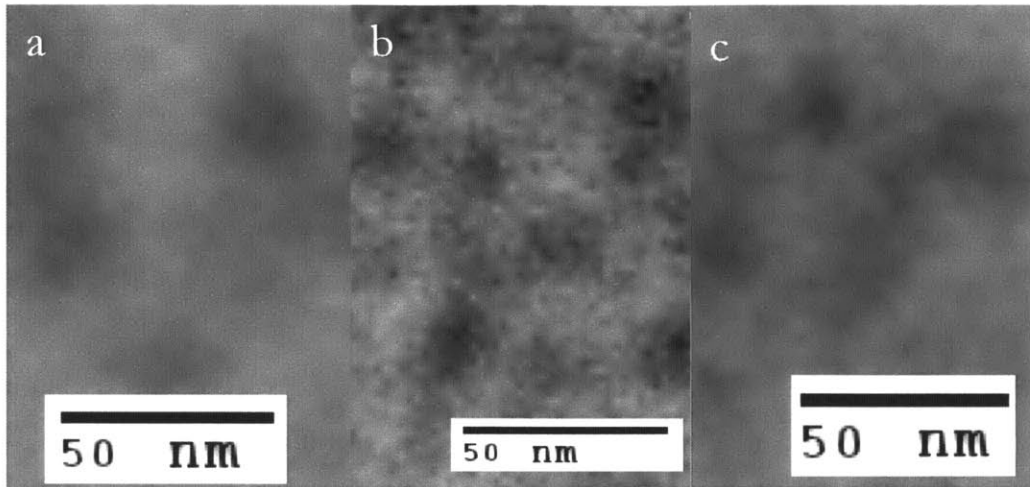


Figure 5. Zoomed in sections from Figure 4 showing the size of stained spots.

3.4. Next Steps

The initial success in cloning up the correct vectors needs to be continued with alternative methods to characterize the proteins and design usable miniSOG barcodes. The MHC-tagged version of miniSOG will probably not work because of its localization exterior to the cytosol, and because of the poor expression results of the construct. There are many ways that cells naturally direct proteins to the membrane, and many of these have been investigated for protein engineering uses. Contrary to the case of MHC, where the protein itself includes a transmembrane domain, many of these mechanisms involve a short (around five amino acid) signal domain at either the N- or C-terminus of a protein that directs a membrane bound molecule to be attached to the protein in the endoplasmic reticulum. Fusions of EGFP with several of these signaling domains were obtained from Daniel Martin Alarcon and tested for expression levels and cell health. Three such anchors were tested—myristoyl²⁸, farnesyl²⁹ and glycosylphosphatidylinositol (GPI)³⁰. Myristoyl is a 14-carbon saturated fatty acid, farnesol is a 15-carbon branched, unsaturated alcohol built from three prenyl groups, and GPI is a more complex glycolipid. All constructs were imaged 12 and 36 hours after transfection with Lipofectamine at 40X magnification and on a confocal microscope. Farnesylated EGFP showed by far the best membrane localization and cell health. Thus a farnesylated miniSOG may be a better approach than pursuing the hybrid between miniSOG and the membrane bound connexin-43 protein.

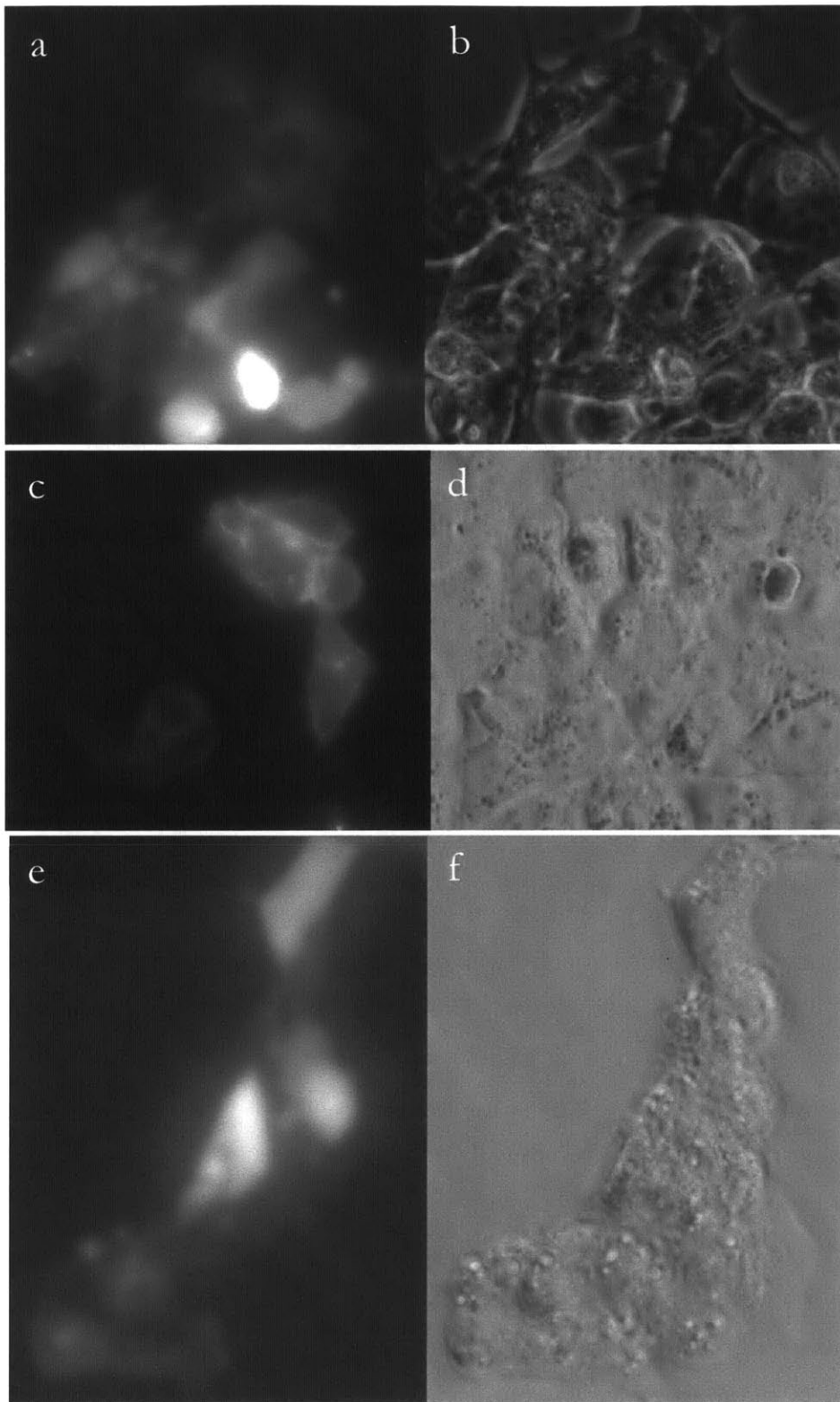


Figure 6. HEK293FT cells expressing EGFP localized to membrane by fusion with signals for myristoylation (a,b), farnesylation (c,d) and attachment of GPI anchor (e,f). Fluorescence is shown in (a,c,e) and bright field in (b,d,f).

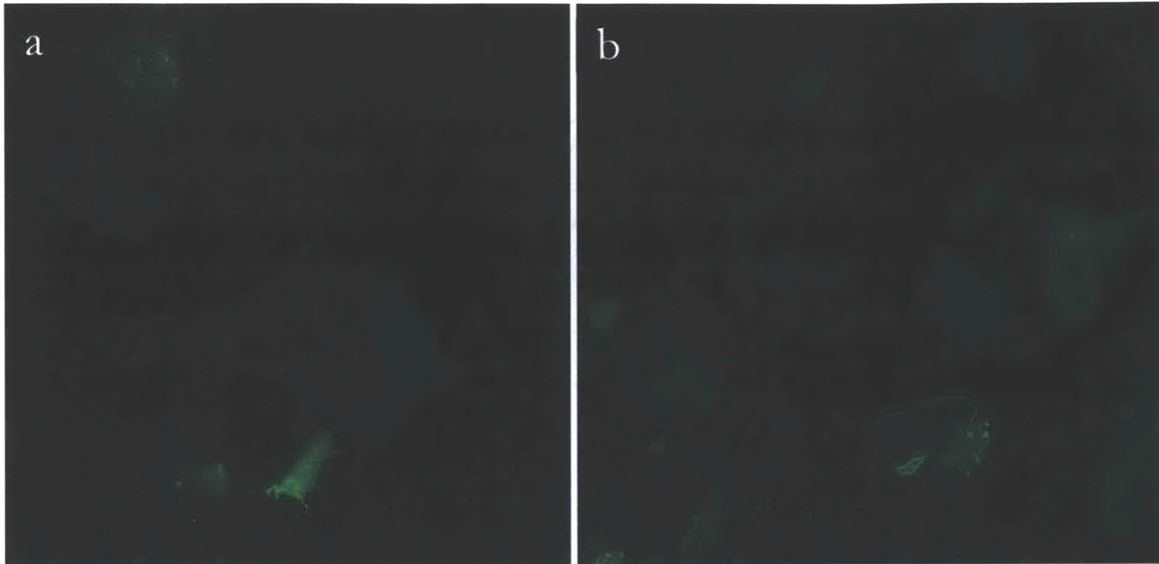


Figure 7. Confocal microscopy of farnesylated (a) and GPI-anchored (b) EGFP.

Alternatively, rather than continuing to work with membrane localized proteins, it may be easier to add a FLAG tag to the existing miniSOG concatamers. A FLAG tag is an eight amino acid sequence against which well-characterized antibodies are available³¹. After photo-oxidation the FLAG-tagged miniSOG can be stained with gold-conjugated anti-FLAG antibodies to give an unambiguous localization of at least a subset of miniSOG proteins. This approach would avoid the problem of baseline staining of other structures in the cell.

One practical problem that has emerged in the course of the electron microscopy study is the low transfection efficiency, coupled with the difficulty of screening through large numbers of cells at the electron microscopy level. This was an especially great problem with the large background signal due to staining of other cellular structures such as ribosomes. During photo-oxidation, the illumination intensity must be as high as possible in order to maximize the signal-to-noise ratio, which means that only small areas of a dish of cultured cells can be oxidized at one time. It would be much easier at the electron microscopy stage if a greater volume of cells could be oxidized and pelleted, resulting in a much higher density of cells in the fully processed specimens. A technique is currently under development to allow the bulk photo-oxidation of such pelleted specimens. In parallel with this effort, concatamers similar to the multi-miniSOGs but using APEX instead of miniSOG will be constructed and tested. Oxidation of DAB by APEX does not require light and thus should

be compatible with a bulk oxidation approach without having to account for light absorption within the specimen and the resulting inhomogeneity in illumination.

4. Highly Multiplexed STORM

The existing STORM-based smFISH technique claims to be readily scalable from 32 to 792 distinct transcripts¹⁶. If achievable, this number is impressive but does not really bring the highly multiplexed smFISH technology from the level of hypothesis testing to a truly unbiased screen of all transcripts. For this reason there is still room for innovation to turn highly multiplexed smFISH into an *in situ*, single cell transcriptomics technology platform.

4.1. Strategies for Transcriptome-Scale smFISH

The central theme of this project is to increase the number of distinguishable fluorophores by using not just spectral information, *i.e.* which fluorophores emit light when pairs of activator and reporter light sources are turned on, but other properties of the fluorophores as well. Fluorophore properties that may be useful for this aim include switching kinetics, bleaching rate, number of photons per switching event, and total number of switching events. With appropriate error correcting codes, these additional axes of information will provide enough distinguishable codes to cover the entire transcriptome.

The first method to generate distinguishable codes using kinetics is to use two different reporters that have similar spectral properties but very different kinetic properties. For example, in the near-IR range both Cy7 and IRDye 800 CW will likely have sufficient performance for this application (achieving the maximum spatial resolution is not necessary since the coding scheme does not rely on the order in which fluorophores appear on each transcript), but IRDye is much more robust against photo bleaching when using a buffer with beta-mercaptoethanol²⁵. In any given frame of imaging these reporters (paired with any given activator), the two alternate reporters will appear identical, but after longer imaging times the Cy7 will have virtually entirely bleached away. The on/off duty cycle of IRDye is six times that of Cy7, giving an additional independent metric for differentiating the two reporters. Likewise in the red-absorbing range, Cy5 and Cy5.5 both produce approximately 5,000 photons per switching event but Cy5.5 has a duty cycle 15 times higher. By keeping track of the fraction of time that each fluorophore is on, these reporters should be distinguishable. The extra IR fluorophore can be paired with five different activators, and

the red with four different activators, yielding a total of 21 distinguishable colors. If each transcript is tagged with a choice of six of these colors, the resulting number of distinguishable codes is 21 choose six, or 54,264.

As an alternative to using different fluorophores, tandem dimers can be explored. For any given reporter, a tandem dimer would be expected to have a doubled switch-on rate. These dimers would also be expected to have accelerated bleaching, as one bleached fluorophore will likely quench its neighbor through a FRET-like transfer of excitation to the bleached molecule's non-radiative recombination pathway³². These features would make monomers and tandem dimers in principle distinguishable. While a single tandem dimer could probably not be distinguished from a single monomer, each transcript is labeled with four copies of each selected activator-reporter pair, increasing the signal-to-noise ratio of this measurement. If each reporter is doubled in this manner, a total of 24 distinguishable reports will be available. If six are chosen for each transcript, the total distinguishable codes is 134,596, leaving room for roughly two bits worth of error correction in the code and still covering a whole human transcriptome. Likewise, the activators can be included in tandem multi-mers to increase the activation rate without changing the mean number of photons produced before bleaching for a given reporter. Finally, the number of probes attached to a transcript with each color can be varied. Doubling the number of, for example, red-emitting activator-reporter pairs would result in twice as many being activated for a given pulse of the activation light, without the accelerated bleaching that is expected to occur for reporter dimers.

4.2. Design and Construction of a STORM Microscope

All work on the STORM microscope and single molecule fluorescence characterization was conducted equally with Fei Chen. The hardware for a STORM microscope has been assembled and aligned. The body is a Nikon Ti-E inverted microscope. The light sources are OBIS lasers from Coherent with wavelengths of 730nm, 648nm, and 555nm, and LEDs from Thorlabs with wavelengths of 470nm and 405nm. Lenses are from Edmund Optics. Filters are from Semrock. Other optical components are from Thorlabs. The camera is an Andor iXon EM-CCD. All laser sources are combined into one beam path by cascading long pass filters. Each filter brings an additional color into the path, with a shorter wavelength than the preceding colors. The LEDs were collimated as much as

possible and integrated into the beam path with two additional long pass filters directly before entering the scope.

In the final design, total internal reflection (TIRF) capability will be included. In TIRF microscopy³³, the fluorescence excitation beam is introduced to the back aperture of the objective off center, so that the beam emerges from the front of the objective at an angle. If this angle is high enough, it will be totally internally reflected at the interface between glass coverslip and the aqueous environment of the specimen. An oil immersion objective is required. As with any example of total internally reflected light, the magnitude of the electric field cannot fall discontinuously to zero on the low index side of the interface. Instead there is a region with an exponentially decreasing field called an evanescent wave that does not carry any energy away as a transmitted beam would. It is analogous to a resonant cavity that can be pumped and can store energy as a standing wave. This wave can nonetheless excite fluorescence. In this arrangement the signal-to-noise ratio for fluorophores within roughly 100nm of the interface is boosted by two features. Firstly, there is no out-of-plane fluorescence excitation (it is also not possible to use this technique to probe deeper than several hundred nanometers past the interface). Secondly, because the wave on the specimen side is a standing wave that does not carry energy away from the interface (except at discrete points due to the presence of fluorophores), the magnitude of the electric field can be several times greater than for a transmitted beam without violating conservation of energy.

TIRF was implemented initially by placing the last section of the beam path on a one-axis translation stage, oriented perpendicular to the beam path entering the back of the microscope. This arrangement was not optimal because while the beam could be successfully steered in this way, it also resulted in the illumination spot moving in specimen plane. As a next step, the translation stage will be removed and replaced with a steering mirror in a conjugate plane to the specimen plane. Thus, the position of the spot in the specimen plane is set by the position in which the beam hits the steering mirror and the angle of the beam emerging from the objective can be controlled independently by the angle of the mirror.

4.3. Single Molecule Fluorescence Characterization

The performance of STORM microscopy depends critically on the chemical properties of the buffer solutions employed, in that they control the blinking and bleaching

kinetics of the fluorophores. In order to test these features of the system, a rapid method to build flow cells was adapted in order to immobilize fluorophore-labeled oligonucleotides onto glass surfaces via a biotin-streptavidin interaction and subject them to a controlled chemical environment³⁴. The glass surface is coated with streptavidin by adsorption of biotin-labeled bovine serum albumin, followed by attachment of streptavidin. Fluorophore blinking has been observed, although the kinetics are not exactly as expected from published results. Depending on the ultimate impact of these deviations on STORM performance buffer conditions may need to be optimized.

STORM activator-reporter fluorophore pairs were constructed using a DNA origami tetrahedron derived from the a design by Mastroianni *et al*⁵. These tetrahedra are constructed with four DNA strands, one for each tetrahedron face. Thus, at any edge there are two DNA strands, which form a double helix, maintaining the shape of the tetrahedron. The tetrahedra are 26 bases, equivalent to about 8nm on a side. At each vertex there is a 5' and a 3' DNA end, which can be decorated with a fluorophore, or extended to produce a single-stranded overhang. In this case, one of the vertices was given an overhang terminated with a biotin, in order to attach to a streptavidin-coated surface. A STORM activator-reporter pair could then be positioned either together on one vertex, or on two adjacent vertices, separated by approximately 8nm. This system provides a good platform for assessing the cross-talk between fluorophores not immediately next to each other.

Data were collected in standard video mode with 200ms exposures. Since the illumination began shortly after the beginning of each video, the first frame with illumination was identified as the one with total intensity exceeding 150% that of the previous frame. The first several (two to five) frames with illumination on were summed up to increase the signal-to-noise ratio, and then the locations of all fluorophores were determined using the object recognition capabilities of the freely available CellProfiler software platform³⁶. The summed intensity for each spot is then collected for each frame of video. Practically all of the fluorophores are expected to be in the on state at the beginning of illumination. For each spot, a threshold is determined using the Matlab built-in Otsu method to determine whether that spot's fluorophore is one or off in each frame. Briefly, the Otsu method works by finding a cutoff to sort the values of a distribution into two buckets that will maximize the goodness of fit if each bucket is modeled as a Gaussian distribution³⁷. This is equivalent to assuming that the original distribution is bimodal, with two underlying populations. Spots

whose goodness of fit values fell below an empirically determined threshold were rejected because these spots tended to include more than one fluorophore, rendering any measurement of their switching kinetics spurious. Figure 8 shows an example of a correct identification of on *vs.* off state of a single Cy5 fluorophore.

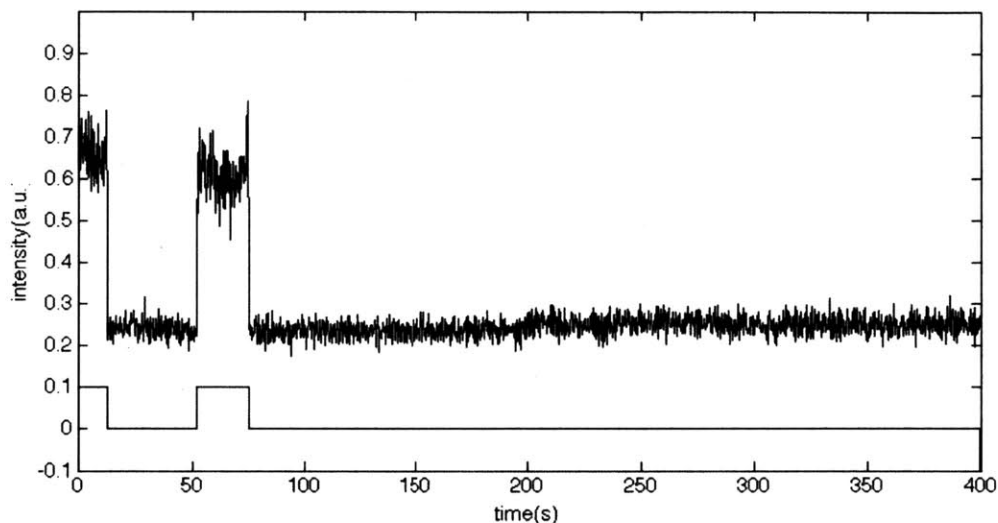


Figure 8. Trace showing measured intensity level and algorithmically determined on/off state of a single fluorophore.

With the on/off state of each fluorophore automatically detected, the total number of fluorophores in the on state was summed up for each frame. A representative plot of the number of fluorophores on in each frame is shown in Figure 9. In this experiment, the reporter is Cy5 and the activator is Alexa 488, activated using a 470nm LED. The large number of fluorophores that are initially on rapidly switch into the dark state, followed by a more gradual rate of permanent bleaching. After 200 seconds, the LED is switched on, reactivating a fraction of fluorophores over a several second span of time, followed by a slower rate of bleaching. When the activation light is switched off, the fluorophores return to their baseline off fraction, at a rate similar to the initial process of blinking off. The baseline is slightly lower due to continued bleaching.

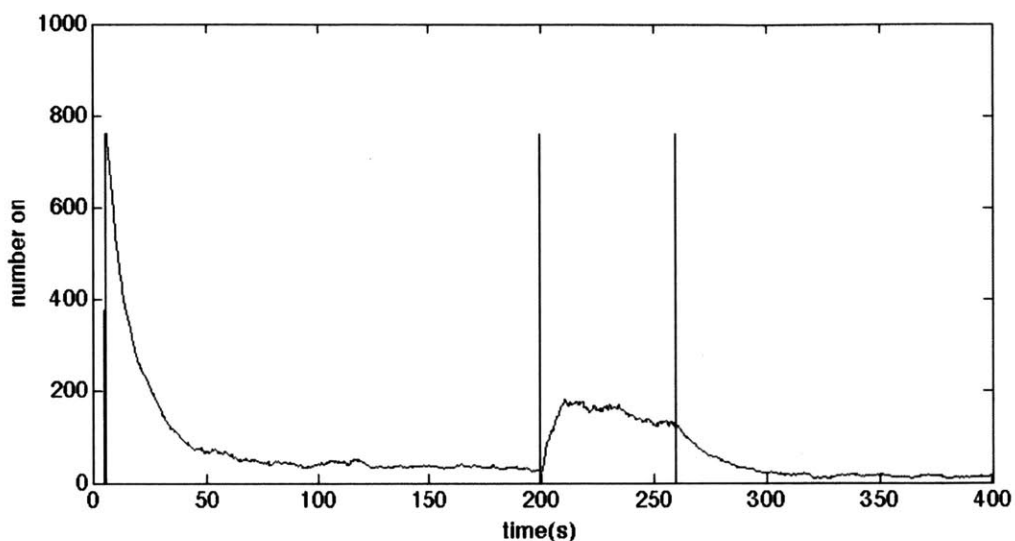


Figure 9. Number of fluorophores detected in on state versus time. Vertical lines indicate time of switching on and off illumination with 470nm LED.

First, the ability of the 470nm LED to activate Cy5 via an Alexa 488 on the same tetrahedron vertex was tested. Each activation trial resulted in a trace similar to that shown in Figure 9. The activation fraction for each trial was defined as the maximum number of fluorophores in the on state during activator illumination divided by the maximum number of fluorophores on during the entire trial. Increasing the LED control voltage from 10mV to 200mV resulted in an activation fraction increasing from 0.07 (which is very close to equilibrium value of fluorophore activation in the absence of activation) to 0.25. Increasing the activation power further did not result in greater activation, indicating a greater than expected level of bleaching had already taken place.

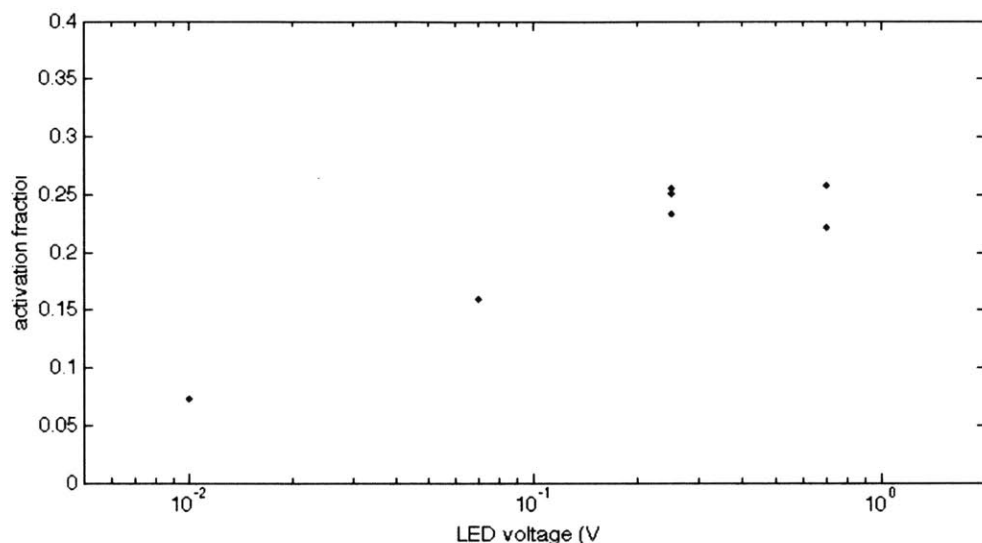


Figure 10. Activation fraction for STORM pair with Alexa 488 as activator and Cy5 as reporter, positioned directly next to each other on the same tetrahedron vertex, activated with 470nm LED at varying control voltages.

The effect of fluorophore proximity was tested by attaching Alexa 405 and Cy5 to the same and to neighboring vertices of tetrahedra. These constructs were activated with a 405nm LED with control voltages of 100mV and 200mV. Results for fluorophores on neighboring vertices are represented as black points in Figure 11, while those for fluorophores on the same vertex are represented in blue. For both power levels, having the activator directly next to the reporter resulted in a greater activation, but the residual activation for neighboring corners using the higher control voltage of 200mV resulted in a considerable activation of the reporter. This level of cross activation would not be acceptable in the context of an experiment. This will be remedied either through optimized buffer conditions or by more greatly separating reporters from activators with which they are not meant to be paired.

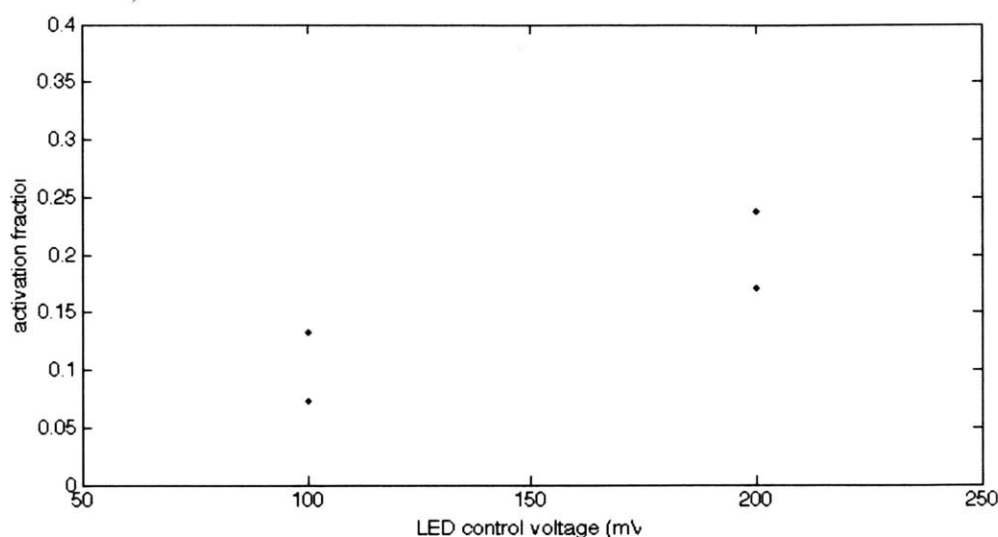


Figure 11. STORM pair with Alexa 405 as activator and Cy5 as reporter positioned either directly next to each other on the same tetrahedron vertex (blue) and on opposite vertices (black), activated with 405nm LED at two control voltages.

5. Conclusion

This work represents the first steps in a project to increase the multiplexing capacity of genetically encoded electron microscopy and the STORM implementation of super resolution optical microscopy. Other investigators have begun to develop the multiplexing potential of STORM, particularly in the area of single molecule FISH. Using the existing STORM colors, however, this technique cannot get past the level of hundreds of transcripts to realize a full measurement of a single cell transcriptome. A STORM microscope has been built with the aim of developing a technique to increase the number of effective colors by measuring the fluorescence kinetic properties in addition to the spectral properties that are currently used to distinguish fluorophores. What remains is to optimize the buffer conditions to recover the fluorophore kinetics expected from the published values.

Several miniSOG concatamers have been produced and expressed successfully in HEK293FT cells. Based on visual inspection the photo-oxidation protocol works correctly. One round of electron microscopy has been done, but the results were not clear. Several fusions of miniSOG with membrane localization tags have been constructed in order to make the electron micrograph analysis unambiguous. This approach may not be the best, however, so several other avenues have been developed and will be attempted in the next steps for this project.

List of Figures

| | |
|--|----|
| Figure 1. HEK293FT cells expressing miniSOG constructs. | 10 |
| Figure 2. HEK293FT cells expressing fusions with connexin43. | 12 |
| Figure 3. Photo-oxidation of 1x-miniSOG. | 13 |
| Figure 4. Transmission electron micrographs of HEK293FT cells expressing miniSOG concatamers..... | 14 |
| Figure 5. Zoomed in sections from Figure 4 showing the size of stained spots..... | 15 |
| Figure 6. HEK293FT cells expressing EGFP localized to membrane..... | 17 |
| Figure 7. Confocal microscopy of membrane-localized EGFP..... | 18 |
| Figure 8. Measured intensity level and on/off state of a single fluorophore..... | 23 |
| Figure 9. Number of fluorophores detected in on state versus time. | 24 |
| Figure 10. Activation fraction for STORM pair with immediately adjacent fluorophores. ... | 25 |
| Figure 11. Activation fraction for STORM pair with separated fluorophores..... | 26 |

Appendix: Methods

1. Transfection and Photo-oxidation of miniSOG

Day 1: Plate cells in 24-well plate

Put 80uL of Matrigel in wells, let stand in cell culture incubator for 30 min.

Aspirate Matrigel.

Within several hours, plate ~20,000 cells per well.

Day 2: Transfect

In 1.5mL tubes, mix reagents: 1.25uL Lipofectamine, 100uL DMEM, 0.5ug DNA, let stand at room temp for 30 min.

Change media, replacing with 500uL of D10.

Add transfection mix drop wise to each well.

Rock plate gently to disperse transfection agent, replace in incubator.

Day 3: Replace media

Aspirate media and replace with 1mL D10 12-36 hours after transfection.

Day 4: Fix and photo-oxidize

Fix:

Prepare 4% formaldehyde in 1x PBS (Gibco, cat. no. 70011-044).

Aspirate wells and add 200uL of 4% formaldehyde, let stand 20 min at room temp.

Wash 3x with 1x PBS.

Make DAB solution:

Dissolve 10mg DAB-4HCl (Sigma cat. no. D5637-1G) in 10mL 1x PBS.

Photo-oxidize:

Replace D10 with 300uL DAB solution.

Search for area with high number of easily distinguishable fluorescent cells, using lowest possible fluorescence excitation. Turn off excitation quickly.

Take bright field photo.

Turn on fluorescence excitation and take photo at $t=0$.

Check bright field image periodically, about once per minute. Stop illumination once oxidation product appears in formerly fluorescent cells, about ten minutes.

2. Transfection with Calcium Phosphate

Seed the cells at a density of 6×10^4 cells/cm² in media with no antibiotics and keep in a humidified incubator (with 5 % CO₂) for a period of 12-14 hours at 37°C. Surface area of 24-well plates – 2 cm².

Coat surfaces with Matrigel (BD, 356230). Dilute Matrigel stock 50-fold in cold DMEM (Gibco). Store at 4°C. To coat glass coverslips in 24-well plates, add 75 µl of diluted Matrigel. For 96-well plates, add 35 µl per well. Incubate 1 hr in incubator.

The next day, pre-warm the ddH₂O, calcium chloride and 2xHBS to room temperature prior to the procedure. Note: The volumes indicated below are for 24-well plates in which cells have been seeded in 500 µl media. For 96-well plates, use 50 µl media and scale everything accordingly.

Add the following together to make the transfection mix: 1.25 µg DNA + 3.125 µl 2 M CaCl₂ solution + ddH₂O to make a final volume of 25 µl. Add this solution to 25 µl of 2xHBS, mix promptly and let it stand for 30 seconds. For low copy transfection (down to one copy per cell on average), dilute plasmid with pUC18 (Agilent Genomics) at 1:100 mass ratio.

Add the transfection mix to the cell media drop wise.

Incubate cells in a humidified incubator (with 5 % CO₂) for a period of 24 hours at 37°C.

Aspirate the transfection mix and replace with fresh media with no antibiotics.

Incubate cells in a humidified incubator (with 5 % CO₂) for a period of 24 - 36 hours at 37°C.

Solutions used (Make new solutions every month):

2 M CaCl₂ solution in ddH₂O. (Store at -20°C). For 50 ml volume add 14.7 g CaCl₂

2X HBS – 50 mM HEPES , 280 mM NaCl, 1.5 mM Na₂HPO₄, pH 7.0 precisely. (Store at -20°C). For 50 ml volume add 0.65 g HEPES, 0.8 g NaCl, 0.02g Na₂HPO₄·7H₂O. Since Na₂HPO₄ concentration is critical, make a 1.5 M stock solution and dilute it to be accurate.

References

1. Levsky, J. M. J. & Singer, R. H. R. Fluorescence in situ hybridization: past, present and future. *J Cell Sci* **116**, 2833–2838 (2003).
2. Nederlof, P. M. *et al.* Multiple fluorescence in situ hybridization. *Cytometry* **11**, 126–131 (1990).
3. Heim, R. & Tsien, R. Y. Engineering green fluorescent protein for improved brightness, longer wavelengths and fluorescence resonance energy transfer. *Curr. Biol.* **6**, 178–182 (1996).
4. Lansford, R., Bearman, G. & Fraser, S. E. Resolution of multiple green fluorescent protein color variants and dyes using two-photon microscopy and imaging spectroscopy. *J Biomed Opt* **6**, 311–318 (2001).
5. Shu, X. *et al.* A genetically encoded tag for correlated light and electron microscopy of intact cells, tissues, and organisms. *PLoS Biol.* **9**, e1001041 (2011).
6. Martell, J. D. *et al.* Engineered ascorbate peroxidase as a genetically encoded reporter for electron microscopy. *Nat. Biotechnol.* – (2012).doi:10.1038/nbt.2375
7. Rust, M. J., Bates, M. & Zhuang, X. Sub-diffraction-limit imaging by stochastic optical reconstruction microscopy (STORM). *Nat. Methods* **3**, 793–795 (2006).
8. Vaughan, J. C., Jia, S. & Zhuang, X. Ultrabright photoactivatable fluorophores created by reductive caging. *Nat. Methods* **9**, 1181–1184 (2012).
9. Yi, H., Leunissen, J. L. M., Shi, G. M., Gutekunst, C. A. & Hersch, S. M. A Novel Procedure for Pre-embedding Double Immunogold-Silver Labeling at the Ultrastructural Level. *Journal of Histochemistry & Cytochemistry* **49**, 279–283 (2001).
10. Bleher, R., Kandela, I., Meyer, D. A. & Albrecht, R. M. Immuno-EM using colloidal metal nanoparticles and electron spectroscopic imaging for co-localization at high spatial resolution. *J Microsc* **230**, 388–395 (2008).
11. Pei, L. *et al.* Uncoupling the dopamine D1-D2 receptor complex exerts antidepressant-like effects. *Nat. Med.* **16**, 1393–1395 (2010).
12. Zhang, J. & Diamond, J. S. Distinct perisynaptic and synaptic localization of NMDA and AMPA receptors on ganglion cells in rat retina. *J. Comp. Neurol.* **498**, 810–820 (2006).
13. Kaufman, A. M. *et al.* Opposing Roles of Synaptic and Extrasynaptic NMDA Receptor Signaling in Cocultured Striatal and Cortical Neurons. *J. Neurosci.* **32**, 3992–4003 (2012).
14. Kerr, J. M. & Blanpied, T. A. Subsynaptic AMPA receptor distribution is acutely regulated by actin-driven reorganization of the postsynaptic density. *J. Neurosci.* **32**, 658–673 (2012).
15. Clarkson, A. N. Perisynaptic GABA Receptors The Overzealous Protector. *Adv Pharmacol Sci* **2012**, 708428 (2012).
16. Lubeck, E. & Cai, L. Single-cell systems biology by super-resolution imaging and combinatorial labeling. *Nat. Methods* **9**, 743–748 (2012).
17. Hashimshony, T., Wagner, F., Sher, N. & Yanai, I. CEL-Seq: single-cell RNA-Seq by multiplexed linear amplification. *Cell Rep* **2**, 666–673 (2012).
18. Femino, A. M., Fay, F. S., Fogarty, K. & Singer, R. H. Visualization of single RNA transcripts in situ. *Science* **280**, 585–590 (1998).
19. Migneault, I., Dartiguenave, C., Bertrand, M. J. & Waldron, K. C. Glutaraldehyde: behavior in aqueous solution, reaction with proteins, and application to enzyme crosslinking. *BioTechniques* **37**, 790–6– 798–802 (2004).

20. Maunsbach, A. B. & Afzelius, B. *Biomedical Electron Microscopy*. (1999).
21. Li, J., Wang, Y., Chiu, S.-L. & Cline, H. T. Membrane targeted horseradish peroxidase as a marker for correlative fluorescence and electron microscopy studies. *Front Neural Circuits* **4**, 6 (2010).
22. Willig, K. I., Rizzoli, S. O., Westphal, V., Jahn, R. & Hell, S. W. STED microscopy reveals that synaptotagmin remains clustered after synaptic vesicle exocytosis. *Nature* **440**, 935–939 (2006).
23. Yildiz, A. & Selvin, P. R. Fluorescence imaging with one nanometer accuracy: application to molecular motors. *Acc. Chem. Res.* **38**, 574–582 (2005).
24. Bates, M. M., Dempsey, G. T. G., Chen, K. H. K. & Zhuang, X. X. Multicolor super-resolution fluorescence imaging via multi-parameter fluorophore detection. *Chemphyschem* **13**, 99–107 (2012).
25. Dempsey, G. T. G., Vaughan, J. C. J., Chen, K. H. K., Bates, M. M. & Zhuang, X. X. Evaluation of fluorophores for optimal performance in localization-based super-resolution imaging. *Nat. Methods* **8**, 1027–1036 (2011).
26. Best, R. B. *et al.* Effect of flexibility and cis residues in single-molecule FRET studies of polyproline. *P Natl Acad. Sci Usa* **104**, 18964–18969 (2007).
27. Gibson, D. G. *et al.* Enzymatic assembly of DNA molecules up to several hundred kilobases. *Nat. Methods* **6**, 343–345 (2009).
28. Resh, M. D. Fatty acylation of proteins: new insights into membrane targeting of myristoylated and palmitoylated proteins. *Biochim. Biophys. Acta* **1451**, 1–16 (1999).
29. Choy, E. *et al.* Endomembrane trafficking of ras: the CAAX motif targets proteins to the ER and Golgi. *Cell* **98**, 69–80 (1999).
30. Paulick, M. G. & Bertozzi, C. R. The glycosylphosphatidylinositol anchor: a complex membrane-anchoring structure for proteins. *Biochemistry* **47**, 6991–7000 (2008).
31. Einhauer, A. & Jungbauer, A. The FLAG peptide, a versatile fusion tag for the purification of recombinant proteins. *J. Biochem. Biophys. Methods* **49**, 455–465 (2001).
32. Luchowski, R. *et al.* Single molecule studies of multiple-fluorophore labeled antibodies. Effect of homo-FRET on the number of photons available before photobleaching. *Curr Pharm Biotechnol* **9**, 411–420 (2008).
33. Reichert, W. M. & Truskey, G. A. Total internal reflection fluorescence (TIRF) microscopy. I. Modelling cell contact region fluorescence. *J Cell Sci* **96 (Pt 2)**, 219–230 (1990).
34. Roy, R., Hohng, S. & Ha, T. A practical guide to single-molecule FRET. *Nat. Methods* **5**, 507–516 (2008).
35. Mastroianni, A. J., Claridge, S. A. & Alivisatos, A. P. Pyramidal and Chiral Groupings of Gold Nanocrystals Assembled Using DNA Scaffolds. *J. Am. Chem. Soc.* **131**, 8455–8459 (2009).
36. Carpenter, A. E. *et al.* CellProfiler: image analysis software for identifying and quantifying cell phenotypes. *Genome Biol* **7**, R100 (2006).
37. Otsu, N. A threshold selection method from gray-level histograms. *Automatica* (1975).